SEA LEVEL ANOMALY AND DYNAMIC OCEAN TOPOGRAPHY ANALYTICAL COVARIANCE FUNCTIONS IN THE MEDITERRANEAN SEA FROM ENVISAT DATA

G.S. Vergos[(1)], D.A. Natsiopoulos[(2)], I.N. Tziavos[(3)]

[(1)]*Aristotle University of Thessaloniki, Department of Geodesy and Surveying, Thessaloniki, GR-54124, Greece, vergos@topo.auth.gr*

[(2)]*Aristotle University of Thessaloniki, Department of Geodesy and Surveying, Thessaloniki, GR-54124, Greece, anatsiopoulos@hotmail.com*

[(3)]*Aristotle University of Thessaloniki, Department of Geodesy and Surveying, Thessaloniki, GR-54124, Greece, tziavos@topo.auth.gr*

ABSTRACT

Monitoring and understanding of sea level change at various spatial and temporal scales have been the focus of many studies during the past decades. The advent of satellite altimetry and the realization of the GRACE/GOCE missions offer new opportunities for the estimation of sea level trends with heterogeneous data combination methods. In related studies, even though the data combination and processing strategies have been carried out carefully with proper control, error propagation through analytical data variance-covariance matrices has been given little attention. The latter is of importance since it can provide reliable estimates of the output signal error. This is especially evident in e.g., least-squares collocation (LSC), where analytical covariance function models for the disturbing potential, its second order derivatives and geoid heights are used. Analytical covariance models are not available for altimetric sea level anomalies making their incorporation in LSC-based combination schemes problematic. This work presents some new ideas and results on the determination of analytical covariance functions for the sea level anomalies in the Mediterranean Sea. The focus is based on single-mission altimetry data from ENVISAT for the entire duration of the mission (2002-2011). The estimation of the analytical covariance functions is performed using 2nd and 3rd order Gauss-Markov models, exponential ones, as well as a kernel similar to that of the disturbing potential. The analysis is carried out in order to come to some conclusions on the SLA spectral characteristics based on empirically derived properties.

Keywords: Satellite altimetry, covariance functions, SLA, DOT, empirical and analytical models.

1. INTRODUCTION

Variations in the sea level and changes at global and regional scales are triggered by a number of factors that take place within system Earth. These natural processes originate from variations in the physical properties of the ocean water and from water mass transport between the Earth's oceans, continents and the atmosphere. Both steric and non-steric (eustatic) sea level variations and their proper modeling play a crucial role not only to oceanographic but geodetic applications as well. The former are due to variations in salinity and temperature, and the latter due to river run-off, glacial and ice caps mass variations and atmospheric water vapor changes [3]. Their proper modeling in terms of data combination and error propagation is essential in marine geoid modeling and Dynamic Ocean Topography (DOT) determination [9]. This is especially evident during the last decade with the advent of the gravity-field dedicated satellite missions of GRACE and GOCE, which allow the combined use of gravity field parameters with satellite altimetry observations to study the Earth's oceans [1, 17].

Since the early 80's, altimeters on-board satellites resulted in the availability of sea surface height measurements with global coverage, homogeneous accuracy and resolution. Satellite altimetry and the multitude of unprecedented in accuracy and resolution observations that it allows precise determinations of sea level variations without the limitations of ground-based observations [2]. Nowadays, the available 20-year record of observations for the sea level together with GRACE/GOCE observables offer new opportunities for the estimation of sea level trends at regional and global scales and the identification of seasonal signals. In such studies, even though the data combination and processing strategies have been carried out carefully with proper control [6, 7], a point that has been given little attention is error propagation through analytical data variance-covariance matrices. Recent examples of studies, where such attempts have been made for the determination of the DOT can be found in [8] and [10] for the region between Greenland and the UK. Rigorous modeling of the signal and error characteristics is of significant importance in heterogeneous data combination studies, since error propagation can provide reliable estimates of the output signal error. This becomes a necessity in the optimal estimator used in physical geodesy, i.e., least-squares collocation (LSC), where the full variance-covariance matrices are needed for the input data and signals to be predicted [16, 17]. When the aim is the determination of sea level variations or the DOT from a combination of altimetric

and GRACE/GOCE observations, one can determine analytical covariance functions for the disturbing potential, its second order derivatives and geoid heights through one of the standard models, as, e.g., that of [13]. On the other hand, no global or regional analytical models are available for altimetric sea level anomalies (SLAs) making their incorporation in LSC-based combination schemes problematic. The main objective of this work is on the proper modeling of available SLA data in order to determine empirical and analytical covariance functions, so that they will subsequently used for prediction with LSC. From the available analytical covariance functions the full variance-covariance matrices of the functional under study, i.e., the SLA or the DOT can be derived. The focus is based on single-mission altimetry data from ENVISAT, in the Mediterranean Sea, for the entire duration of the satellite mission (2002-2011). Both along-track (1D) and cross-track (2D) cases are studied interpreting the empirical and modeled characteristics of the covariance functions. For the former, the signal characteristics of the sea level anomalies have been studied at monthly, seasonal and annual scales. The estimation of the analytical covariance functions is performed using 2nd and 3rd order Gauss-Markov models, simple exponential ones as well as a kernel similar to that of the disturbing potential, a.k.a., dependent on a series of Legendre polynomials. From that analysis, which is carried out for the entire Mediterranean, conclusions on the SLA spectral characteristics based on empirically derived properties such as the variance and correlation length are derived, while some conclusions on the annual SLA variability are drawn as well.

2. DATA AND ANALYTICAL MODELS

As already mentioned, the present study is focused in the entire Mediterranean basin, within the region bounded between $30^o \le \varphi \le 50^o$ and $-10^o \le \lambda \le 40^o$. In this region, the statistical characteristics of the SLA have been studied using altimetric observations from ENVISAT for the entire duration of its mission (2002-2011). The ENVISAT data were acquired from the RADS system [12] as SLAs relative to the EGM2008 geopotential model. All geophysical and instrumental corrections have been applied, using the default models proposed by the RADS system, so that corrected SLAs would be available. Given the data availability, two main sets of tests have been carried out for the estimation of SLA analytical covariance functions. The first one refers to the use of a single pass of the satellite, in order to study the stochastic characteristics of the SLA in the along-track (1D) direction. For that case, the longest pass available in the Mediterranean Sea (pass 444) has been chosen (see Fig. 1) in order to utilize as many as possible SLA observations without any interruptions from dry-land areas (islands, isles, etc.). The second test refers to the use of the entire set of ENVISAT passes for the Mediterranean Sea, so that the SLA variability will be studied in both the along- and cross-track (2D) direction (see Fig. 1).

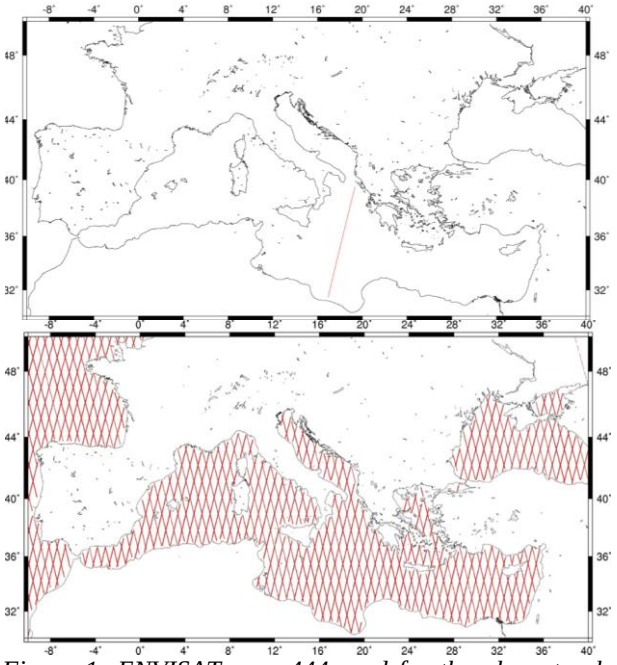

Figure 1: ENVISAT pass 444 used for the along-track (1D) SLA covariance function study (top) and distribution of ENVISAT passes (bottom) in the Mediterranean Sea (2D case).

In order to study the statistical characteristics of the SLA, either in the 1D and the 2D case, first the empirical covariance models were derived. Given a set of observations for the functional $C(\bullet)$ under consideration, in our case the SLA (h^{SLA}), the empirical covariances for a given spherical distance ψ is [4, 12]:

$$\boldsymbol{C}\left(h_i^{SLA},h_j^{SLA},\psi\right)=M\left\{h_i^{SLA}h_j^{SLA}\right\}_{\psi}, \quad (1)$$

where, M denotes the mean value operator and i, j the SLA observations at two points in the area under study with a distance ψ. Employing Eq. 1, the empirical covariance functions for pass 444 have been estimated for all available ENVISAT cycles. Given the 35-day repeat period of ENVISAT, it is implied that for each year ~11 covariance functions have been determined. An example is presented in Fig. 2 (top), where the empirical covariance functions for pass 444 for the year 2005 are depicted. From that figure it is interesting to notice the variability of the variance through the epochs of its year, with high values in January, lower values in spring due to reduced rainfall, increasing values as summer progress due to snow melt and the thermal expansion in July-August. Finally, the variance values decrease again in fall and start increasing in November due to higher level of precipitation. This evolution through time is shown in the Fig. 2 (bottom), where the variances, i.e., the covariance for spherical distance $\psi=0$, between 2002 and 2010 are presented. It is clear

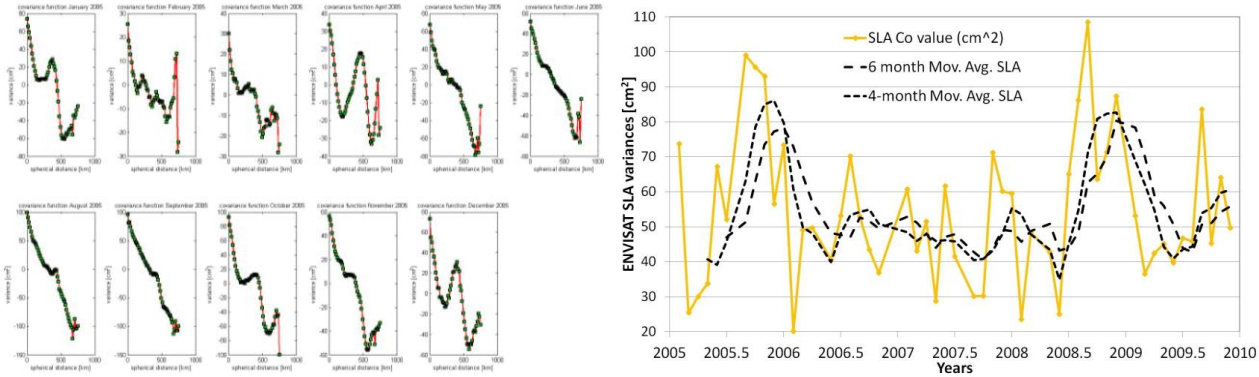

Figure 2: ENVISAT pass 444 empirical covariance functions for 2005 (left) and variance variability for the period under study (right).

that cyclo-stationarity is evidenced, showing the repeated behavior of the SLA variations with epochs. The abnormal behavior is correlated with ENSO events, e.g., overall low in January 2006 and overall high in August 2008. It is interesting to notice that the low in January 2006 is a response to the La-Niña event in September 2005, i.e., with a time lag of 4-5 months, while the high in August 2008 is a response to the negative Southern Oscillation Index (SOI) in April 2008.

In order to determine some analytical model for the SLA covariance function, various options have been tested. The first class of analytical models refers to exponential ones, where six choices were examined, with varying number of parameters to be determined, as follows:

$$\boldsymbol{C}_{h^{SLA}h^{SLA}}(\psi) = \alpha e^{b\psi}, \tag{2}$$

$$\boldsymbol{C}_{h^{SLA}h^{SLA}}(\psi) = \alpha e^{b\psi} + ce^{d\psi}, \tag{3}$$

$$\boldsymbol{C}_{h^{SLA}h^{SLA}}(\psi) = \alpha e^{-\left(\frac{\psi-b}{c}\right)^2}, \tag{4}$$

$$\boldsymbol{C}_{h^{SLA}h^{SLA}}(\psi) = \alpha e^{-b\psi^2}, \tag{5}$$

$$\boldsymbol{C}_{h^{SLA}h^{SLA}}(\psi) = \alpha e^{-b\psi}\cos(\omega\psi), \tag{6}$$

$$\boldsymbol{C}_{h^{SLA}h^{SLA}}(\psi) = \alpha(1+b\psi)e^{-b\psi}. \tag{7}$$

In Eqs. 2-7, *a*, *b* and *c* denote parameters to be determined so that the analytical covariance model will fit the empirical one. Note that all above models are a function of the spherical distance between the points where SLA observations exist. Those six models will be denoted as MODEL A, B, …, F, respectively in the sequel. The other class of analytical models tested refers to 2nd and 3rd order Gauss-Markov ones (MODEL G and H herein) as outlined in Eqs. 8 and 9 respectively, where *D* is the characteristic distance, *r* is the planar distance and $\sigma^2_{h^{SLA}}$ the SLA variance [5, 15]

$$\boldsymbol{C}_{h^{SLA}h^{SLA}}(r) = \sigma^2_{h^{SLA}}\left(1+\frac{r}{D}\right)e^{\left(-r/D\right)}, \tag{8}$$

$$\boldsymbol{C}_{h^{SLA}h^{SLA}}(r) = \sigma^2_{h^{SLA}}\left(1+\frac{r}{D}+\frac{r^2}{3D^2}\right)e^{\left(-r/D\right)}. \tag{9}$$

Finally, an analytical model similar to the one used by [14] for the disturbing potential has been tested. In complete analogy, we can define the covariance function of the SLA or the DOT as (MODEL I herein):

$$\boldsymbol{C}_{h^{SLA}h^{SLA}}(\psi) = \sum_{n=0}^{\infty}\sigma_n^2\left(h^{SLA}\right)P_n(\cos\psi), \tag{10}$$

where $\sigma_n^2\left(h^{SLA}\right)$ are the degree variances of the SLA and $P_n(\cos\psi)$ the Legendre polynomials. Note that in all cases the analytical covariance function models should agree to the empirical values available for the area under study in order to represent the local statistical characteristics of the signal under consideration, i.e., the SLA in this case. For the description of the behavior of the degree variances given in Eq. 10 a 3rd degree Butterworth filter is used so that the degree variances of the SLA are given as [10]:

$$\sigma_n^2\left(h^{SLA}\right) = b\left(\frac{k_2^3}{k_2^3+n^3}+\frac{k_1^3}{k_1^3+n^3}\right)s^{n+1}. \tag{11}$$

The factors *b*, k_1, k_2 and *s* are determined so that the analytic model fits the empirical values describing the statistical characteristics of the functional in the area under study and more precisely the variance and the correlation length. Note that the scale factor s^{n+1} in Eq. 11 resembles the $(R_B/R)^{2(n+1)}$ one in the Tscherning and Rapp analytical covariance model of the anomalous potential. As far as the study of the statistical characteristics of the DOT is concerned, from the various models available the one chosen in the present study is that by [14].

3. SLA ANALYTICAL MODELS AND ACCURACY

All aforementioned models have been evaluated first in the 1D case, where the empirical covariance function for ENVISAT pass 444 was estimated for the entire duration of the mission (2002-2011). The results

presented below refer to a single month of the satellite data (August 2005) in order to demonstrate the performance of the analytical models. Within the estimation strategy followed, first the empirical covariance function is determined, then the analytical models are fitted to the empirical values and finally, prediction is carried out with LSC in order to evaluate the accuracy that they offer. Three tests are performed, the first one by omitting the first 20 records of the track and using the rest for the prediction (TEST 1), the second by omitting the last 20 points (TEST 2) and the third by omitting every second point (TEST 3) and using the rest for the prediction. The tests cases are also depicted with the boxes in Fig. 3, where the SLA for August 2005 and the sub-satellite points for pass 444 are displayed. In Fig. 3 the empirical covariance function of the SLA is depicted with red dots, along with the fitted analytical models (Models A, B, …, F, I). From Fig. 3, the exponential models seem to provide a good fit to the empirical values, as the Gauss-Markov models do. The only model that seems to miss-model the empirical one is the one based on the expansion of Legendre polynomials (MODEL I), probably due to the limited number of observations and the limited extent of the area under study. Tab. 1 summarizes the statistics of the ENVISAT pass 444 for August 2005 along with the prediction errors from the various analytical models for all three test cases (TEST A: prediction in the first 20 points from the rest, TEST B: prediction in the last 20 points from the rest and TEST C: prediction every second point from the rest). As far as TEST A is concerned, the exponential model E and the second order Gauss-Markov models provide the best results with a standard deviation of the prediction errors at the ±8.7 cm. It is noticing that between the two, the Gauss-Markov model provides a mean value smaller 7 cm compared to the exponential one, which is positive in terms of the estimation of unbiased errors. The parameters estimated for model E were $a=90.47\ cm^2$ and $b=0.015\ 1/^o$, while for the 2nd order Gauss-Markov $\sigma^2_{h^{SLA}} = 87.39\,cm^2$ and $D=115.32\ km$ (see Eqs. 6 and 8). The same behavior is evidenced from the results for TEST B, where the exponential models E and F along with the second order Gauss-Markov model gave the most rigorous prediction errors, with a std at the ±5.5-5.9 cm level. From these two tests, which simulate the case where SLA data from altimetry need to be predicted close to the coastline, the performance of the third order Gauss-Markov and that of the expansion in Legendre polynomials present the largest errors. Almost all analytical models perform well in TEST C giving small errors of the order of a few cm (±1.95-2.18 cm) and mean values at the sub-mm level. MODEL I does not perform well again giving a standard error of ±4.5 cm. The improvement is due to the existence of more data in the region where predictions need to be made.

As far as the 2D case is concerned, two tests have been carried out. One using a complete cycle of the ENVISAT data for the entire Mediterranean Sea (all passes included, see Fig. 1 bottom). This consisted of a total number of 11870 SLA observations, for which analytical covariance functions were determined and predictions were made by omitting every second point and using the rest to estimate the SLA in these locations (TEST D in the sequel). The second test refers to using the entire set of ENVISAT data, to predict SLA at an inner window where no observations are available. The inner window was selected for the area bounded between ($32^o \le \varphi \le 36^o$ and $15^o \le \lambda \le 20^o$). This resembles the case when no information is available in a

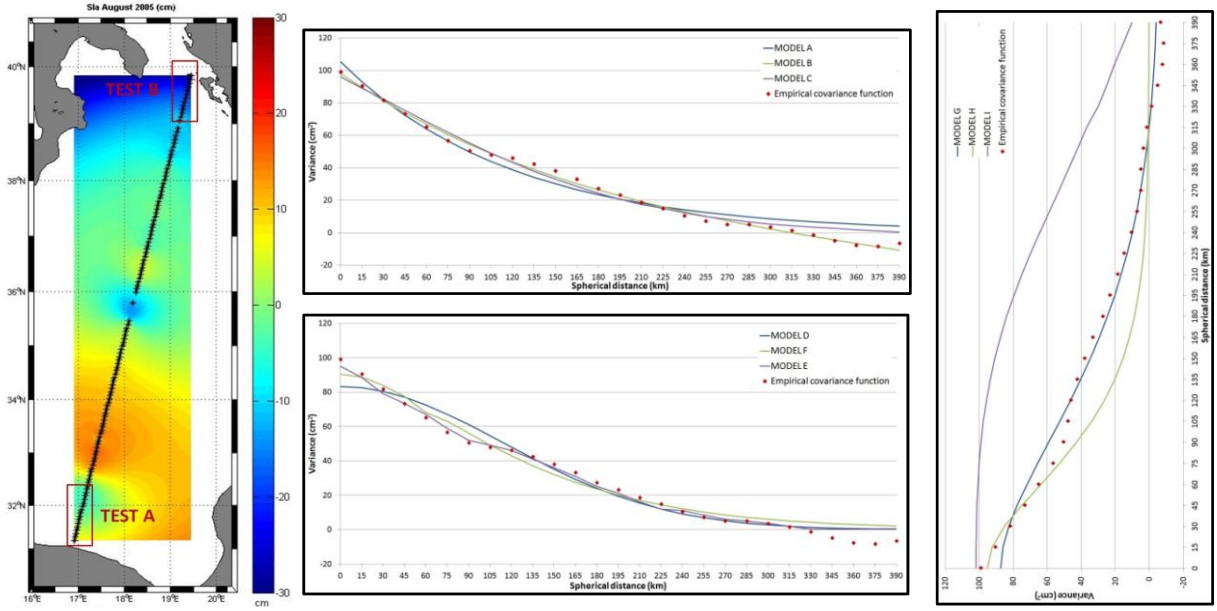

Figure 3: ENVISAT SLA along pass 444 (left) and empirical and analytical model covariance functions (right).

Table 1: Statistics of the ENVISAT pass 444 SLAs and prediction errors from the various analytical models for all test cases investigated. Unit: [cm].

	min	max	mean	std
SLA	-19.9	23.5	7.4	±8.5
TEST A				
MODEL A	-29.07	3.74	-10.06	±8.87
MODEL B	-18.60	5.07	-4.02	±6.10
MODEL C	-27.75	4.46	-8.53	±8.75
MODEL E	-27.66	4.53	-8.63	±8.67
MODEL F	-22.22	9.53	-0.84	±9.39
MODEL G	-18.97	11.47	1.69	±8.70
MODEL H	-20.76	22.48	7.27	±12.88
MODEL I	-91.3	-2.70	-35.65	±32.5
TEST B				
MODEL A	-13.39	5.95	-6.13	±5.54
MODEL B	-128.22	-10.89	-78.97	±35.41
MODEL C	-13.55	6.57	-5.99	±5.78
MODEL E	-13.74	6.38	-6.23	±5.78
MODEL F	-10.57	8.86	-3.15	±5.54
MODEL G	-10.19	10.42	-2.24	±5.94
MODEL H	-15.40	5.79	-7.73	±6.31
MODEL I	22.36	79.54	30.72	±28.59
TEST C				
MODEL A	-7.61	5.08	-0.11	±1.99
MODEL B	-7.57	5.10	-0.06	±1.88
MODEL C	-7.52	5.09	-0.10	±1.95
MODEL D	-86.59	17.39	-1.43	±12.47
MODEL E	-7.55	5.09	-0.10	±1.95
MODEL F	-8.98	5.27	-0.08	±2.07
MODEL G	-9.00	5.27	-0.07	±2.07
MODEL H	-9.94	5.29	-0.08	±2.18
MODEL I	-11.58	10.37	-0.08	±4.57

specific area and LSC is used for the prediction. The validation is performed through comparisons with the available observations (TEST E in the sequel). Once again, the empirical covariance functions have been estimated and the analytical models were fitted, carrying out predictions using these fitted values. Fig. 4 presents the empirical and analytical (for Models G & H) covariance functions for the case investigated in TEST D. The parameters estimated for the 2nd order Gauss-Markov were $\sigma^2_{h^{SLA}} = 85.28 cm^2$ and *D=268.11 km* in the case of TEST D, and $\sigma^2_{h^{SLA}} = 43.81 cm^2$ and *D=34.81 km* in the case of TEST E.

Table 2, summarizes the results for the prediction errors estimated in TEST D & TEST E for a selection of the available analytical models. From Tab. 2 the outperformance of the exponential model E and that of the Gauss-Markov models are evident, with a std at the ±3.6-4.5 cm level and a mean which is close to zero. The range of the Gauss-Markov models is larger by ~40 cm compared to that of the exponential models, signaling that in wider areas, planar analytical models cannot provide rigorous estimates. In TEST E, where an entire window within the study area is missing, all models give disappointing results, since the smallest std of the prediction errors is ±7.39 cm (MODEL E) when the std of the original field is ±7.50 cm. This is due to the fact that the area where predictions are made is quite large ($4^o \times 5^o$), so that the rest of the data cannot describe the SLA variability. The same analysis has been carried out for the DOT model of Rio (see Fig. 4, right). From the analysis carried out, MODEL E and MODEL F provided once again the best results with a prediction error at the ±4.56 cm level and a mean value of the order of 0.5-1 cm.

Table 2: Statistics of prediction errors from the various analytical models for TEST D and TEST E. Unit: [cm].

	min	max	mean	std
TEST D				
SLA	-50.90	55.40	7.33	±11.49
MODEL A	-34.88	29.31	-0.03	±3.65
MODEL B	-34.88	29.37	-0.03	±3.65
MODEL E	-34.89	29.39	-0.03	±3.65
MODEL F	-47.95	55.15	-0.02	±4.57
MODEL G	-47.97	55.18	-0.02	±4.57
MODEL H	-80.37	89.49	-0.02	±5.77
TEST E				
SLA	-44.80	19.80	0.04	±7.50
MODEL A	-30.91	29.50	0.19	±7.40
MODEL E	-30.91	29.50	0.19	±7.39
MODEL G	-403.55	234.2	1.03	±34.63

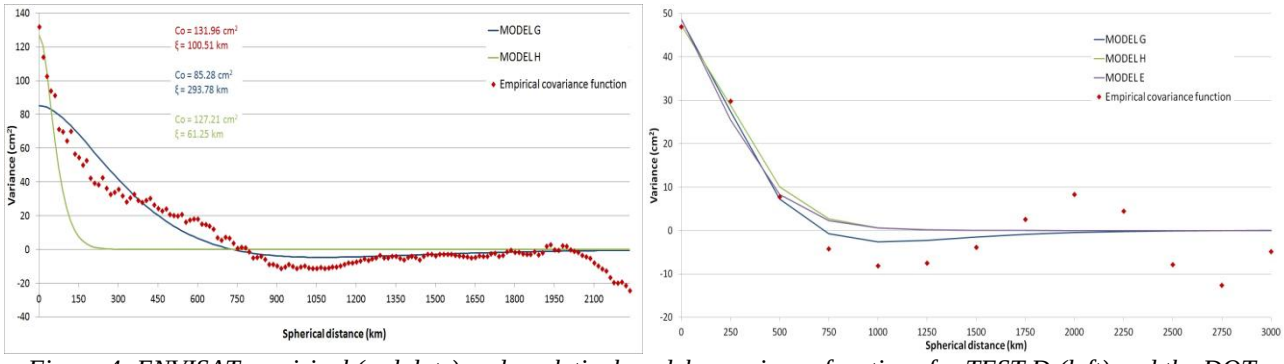

Figure 4: ENVISAT empirical (red dots) and analytical model covariance functions for TEST D (left) and the DOT (right).

4. CONCLUSIONS

A comprehensive analysis on the determination of analytical covariance functions for the SLA has been presented, employing various models, both planar and spherical ones. The tests performed refer to both along-track (1D) and cross-track (2D) cases, where LSC has been used to estimate the SLA either for prediction close to the coastline and to fill-in gaps. From all tests carried out, the exponential model (Model E) and the 2nd order Gauss-Markov one provided the most rigorous results in terms of prediction accuracy (std and mean value of prediction errors), which were at the few cm level. For all cases, the parameters of the analytical covariance models have been determined so that they fit the empirical values. The results acquired with the model based on the expansion in Legendre polynomials were disappointing, and always inferior to the simpler exponential and Gauss-Markov ones, which is a subject that needs to be investigated further. Some key issues may relate to the scaling factor used, which is estimated within the fit to the empirical values. Future work will be directed to the inclusion of time as a variable in the employed analytical models in order to model the variability of SLA with time with LSC.

ACKNOWLEDGEMENT

This work was carried out in the frame of the ESA-PRODEX GOCESeaComb project (C4000106380).

REFERENCES

1. Barzaghi, R., Tselfes, N., Tziavos, I.N. & Vergos, G.S. (2009). Geoid and High Resolution Sea Surface Topography Modelling in the Mediterranean from Gravimetry, Altimetry and GOCE Data: Evaluation by Simulation. *J. Geod.* **83**(8):751-772.
2. Chelton, D.B., Ries, J.C., Haines, B.J., Fu, L.-L. & Callahan, P.S. (2001). Satellite altimetry. In International Geophysics Series "Satellite Altimetry and Earth Sciences: A Handbook of Techniques and Applications" (Eds. L.-L. Fu & A. Cazenave), Academic Press, San Diego **69**:4-131.
3. Garcia, D., Ramillien, G., Lombard, A. & Cazenave, A. (2007). Steric sea-level variations inferred from combined Topex/Poseidon altimetry and GRACE gradiometry. *Pure Appl. Geophys.* **164**:721-731.
4. Heiskanen, W.A. & Moritz, H. (1967). *Physical Geodesy*. W.H. Freeman, San Fransisco.
5. Jordan, S.K. (1972) Self-Consistent Statistical Models for the Gravity Anomaly, Vertical Deflections, and Undulation of the Geoid. *J. Geophys. Res.* **77**(20):3660-3670.
6. Knudsen, P. (1987). Estimation and modelling of the local empirical covariance function using gravity and satellite altimeter data. *Bull. Geod.* **61**:45-160.
7. Knudsen, P. (1991). Simultaneous estimation of the gravity field and sea surface topography from satellite altimeter data by least-squares collocation. *Geophys. J. Inter.* **104**(2):307-317.
8. Knudsen, P. (1992). Estimation of sea surface topography in the Norwegian sea using gravimetry and Geosat altimetry. *Bull. Géod.* **66**:27-40.
9. Knudsen, P. (1993). Integration of gravity and altimeter data by optimal estimation techniques. In Lecture Notes in Earth Sciences "Satellite Altimetry for Geodesy and Oceanography" (Eds. R. Rummel & F. Sansò), Springer-Verlag, Berlin Heidelberg, **50**:453-466.
10. Knudsen, P. & Tscherning, C.C. (2007). Error Characteristics of dynamic topography models derived from altimetry and GOCE Gravimetry. In IAG Symposia "Dynamic Planet 2005 - Monitoring and Understanding a Dynamic Planet with Geodetic and Oceanographic Tools" (Eds. Tregoning P. & Rizos, C.), Vol.130. Springer Berlin Heidelberg, pp. 11-16.
11. Moritz, H. (1980). *Advanced Physical Geodesy*. Wichmann, Karlsruhe.
12. RADS (2012) Radar altimetry database system, Delft Institute for Earth-Oriented Space research (DEOS), http://rads.tudelft.nl/rads/rads.shtml. [Accessed: January 2012]
13. Rio, M.H. & Hernandez, F. (2004). A mean dynamic topography computed over the world ocean from altimetry, in-situ measurements and a geoid model. *J. Geoph. Res.* **109**(12):C12032
14. Tscherning, C.C. & Rapp, R.H. (1974). Closed covariance expressions for gravity anomalies, geoid undulations, and deflections of the vertical implied by anomaly degree-variance models. Reports of the Department of Geodetic Science, 208, The Ohio State University, Columbus, Ohio.
15. Vassiliou, A.A. (1988) The computation of aliasing effects in local gravity field approximation. *Bull. Geod.* **62**(1):41-58.
16. Vergos, G.S., Tziavos, I.N. & Andritsanos, V.D. (2005). On the determination of marine geoid models by least-squares collocation and spectral methods using heterogeneous data. In International Association of Geodesy Symposia "A Window on the Future of Geodesy" (Ed. F. Sansó), Vol. 128. Springer, pp. 332-337.
17. Vergos, G.S., Tziavos, I.N. & Sideris, M.G. (2012). On the determination of sea level changes by combining altimetric, tide gauge, satellite gravity and atmospheric observations. In International Association of Geodesy Symposia "Geodesy for Planet Earth" (Eds. S. Kenyon, C. Pacino & U. Marti), Vol. 136, Springer, pp. 123-130.